Proceedings of the Australian Society of Sugar Cane Technologists, volume 41, xx-xx, 2019

Peer-reviewed paper

Shredder windage investigation

AP Mann, F Plaza and GA Kent

Queensland University of Technology, Brisbane, Qld 4000; a.mann@qut.edu.au

Abstract Air flow through a shredder is complex. There are many examples where relatively small design changes to the shredder and surrounding conveyors can cause quite large changes to air flow. Windage is the term used to describe undesirable air flow. Windage that is counter current to the flow of cane into the shredder is particularly undesirable because it can cause feeding problems. Windage can limit the transfer of energy from the shredder hammers to the cane billets by reducing the relative velocity at impact which can reduce preparation. Shredder windage is also a source of dust, trash and billet emissions. A computational fluid dynamics model of a shredder has been developed to model the air flow through a shredder and its surrounding conveyors. A subsequent investigation, carried out on two factory shredders that suffered from significant windage, is described. Computational fluid dynamics was used to investigate the windage problem and evaluate potential design solutions. Modifications were made to both shredders. Measurements were carried out on these shredders before and after the modification to validate the model predictions, understand the factors that cause windage and reduce the detrimental effects.

Key words Shredder, computational fluid dynamics, windage, flow measurements

INTRODUCTION

Shredding is the critical first stage of the sugar extraction process. Shredder problems often cause reduced extraction, stoppages and high bagasse moisture contents that disrupt the operation of the boiler station. One of the issues many shredders experience is windage (undesirable air flow that can reduce the transfer of energy from the shredder hammers to the cane billets) and causes emissions of dust, trash and billets.

As part of an earlier investigation into the cane preparation process, computational fluid dynamics (CFD) modelling of the air and particle flows in the Rocky Point Mill shredder was undertaken (Mann *et al.* 2017). This earlier work included air flow measurements from the shredder inlet and outlet chutes to assess the accuracy of the air-flow modelling predictions.

Here, we summarise further developments in modelling and measuring air flows. Air-flow CFD models of the shredders at two factories that have experienced problems with shredder windage, Plane Creek Mill and Tully Mill, were set up. These models were used to predict the air-flow patterns through the shredders before and after design modifications to reduce windage. Air-flow measurements were carried out at both shredders before and after the modifications to assess the effect of the modifications on windage and the accuracy of the model predictions.

BACKGROUND

The hammers on the Plane Creek shredder (2470 mm wide) are arranged in a checkerboard pattern (half complement) with 16 rows of hammers and 13 hammers per row giving a total of 208 hammers. Extensive modifications to the shredder were carried out during the 2018 maintenance season to improve feeding and reduce windage. These modifications included windage plates at the cane inlet and cane outlet, removal of an internal baffle, a modified rotor casing shape, a relocated kicker and a modified feed chute.

The hammers on the Tully Mill shredder (2690 mm wide) are also arranged in a checkerboard pattern (half complement). In previous seasons, the shredder had 168 hammers (12 rows, 14 hammers per row) and this arrangement was modified to increase the number of hammers to 224 (16 rows, 14 hammers per row) prior to the start of the 2018 crushing season. The number of hammers was increased to improve preparation, but a side effect of this change was increased windage. After the installation of an added windage plate at the bottom of the feed chute during the 2018 crushing season, the windage reduced significantly. Figure 1 shows some particles near the cane inlet to the shredder that were made airborne by windage prior to the installation of the added windage plate.

Figure 1. Inlet to the Tully shredder operating prior to the installation of the added windage plate showing particles that were made airborne by windage near the curtain.

PROCEDURE

CFD modelling

The ANSYS Fluent CFD package was used for the air flow modelling of both shredders. This package includes the DesignModeler component, which is used to input the geometry to be modelled, a mesh generator, the Fluent model set up component and the CFD-Post component, which is used to visualise and post-process the results of a CFD analysis.

The simulations of both shredders considered only the air flow patterns; the effects of billets and prepared cane on the air flow distributions were ignored. The k-ε turbulence model (Launder and Spalding 1972) with the realisable and enhanced wall-treatment options was used in all the simulations. Pressure boundary conditions set to atmospheric pressure were used at the inlet and outlet of the modelled flow regions. This type of boundary condition allows the code to predict reverse flow. The modelled rotational speed of both shredders was 1000 r/min and all the faces of the rotating assembly were modelled as rotating boundaries. The rotating assemblies of both shredders (shaft, discs, hammer pivot bars and hammers) were modelled as moving boundaries with no slip. All the simulations carried out were steady state. Both shredder arrangements feature a kicker at the top of the shredder feed-chute that rotates a lot slower than the shredder rotor, so the rotation of the kicker was ignored in the simulations. The kicker tines were not included in the simulations of either shredder (i.e. the kickers were modelled as non-rotating cylinders). To reduce computational requirements, the models of

both shredders only represented a portion (approximately 760 mm) of the respective shredder widths. Symmetry boundary conditions were used on each end of the computational domains for all shredder models.

Plane Creek

Figure 2 shows side elevation views of the DesignModeler representations of the Plane Creek shredder before and after the modifications. The mesh used for the shredder simulations before the modifications had 237,962 nodes and 1,194,036 elements and the mesh used for the shredder simulations after the modifications had 235,344 nodes and 1,181,486 elements. The views in Figure 2 have cane flowing from right to left and anticlockwise rotation of the rotor.

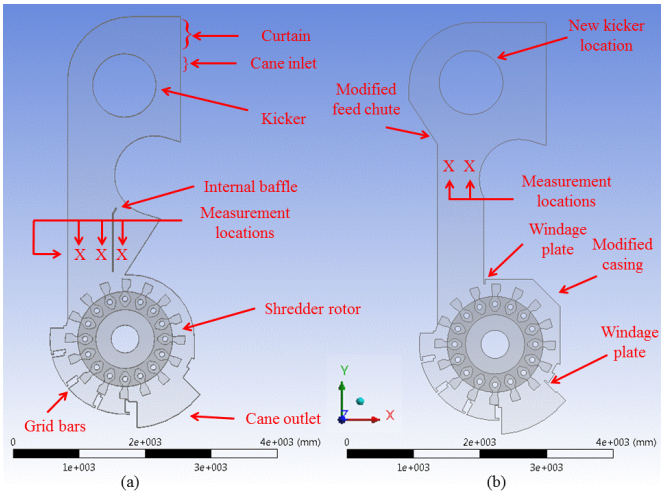

Figure 2. Side-elevation views of the DesignModeler representations of the Plane Creek shredder (a) before and (b) after the modifications.

Tully

A side elevation view of the DesignModeler representation of the Tully shredder set-up with the added windage plate (180 mm length) at the bottom of the inlet chute installed is shown in Figure 3. The simulations without the windage plate used the same flow domain as that shown in Figure 3 except for the added windage plate not being present. The mesh used for the simulations without and with the added windage plate had 584,259 nodes and 3,192,318 elements. The view in Figure 3 has cane flowing from left to right and anticlockwise rotation of the rotor**.** Cane enters on the grid bar side of the Tully shredder and on the cane outlet side of the Plane Creek shredder.

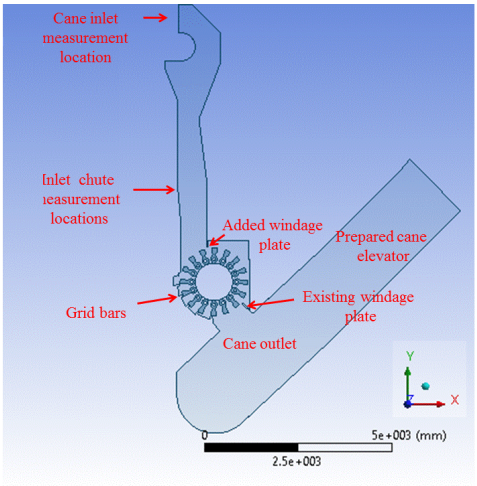

Figure 3. Side-elevation view of the DesignModeler representations of the Tully shredder after the installation of the added 180 mm windage plate at the bottom of the inlet chute.

The Tully shredder has feed rolls, but these rolls were not included in the models of the shredder. A single large outlet on top of the prepared cane elevator chute and the opening to the first mill chute was modelled. The rakes and moving mechanism inside the prepared cane elevator were not modelled.

Measurements

Air velocities and pressures were measured at locations around both shredders with a hot-wire anemometer and a portable pressure meter. To avoid damaging the hot-wire anemometer probe, the measurements had to be taken during short stops when there was steam available to run the shredder turbines but no cane flow. As noted previously (Mann *et al.* 2017), the air flows with cane flow through the shredder are likely to be lower with billets providing extra flow resistance at the entrance to the inlet chute and in the prepared-cane elevator chute. The billets are also like to affect the air flow direction.

Plane Creek

Air velocities were measured from the grid bar side of and one side wall of the inlet chute of the Plane Creek shredder during the 2017 crushing season at the approximate elevation shown in Figure 2(a). Plan views of the velocity measurement locations are shown in Figure 4.

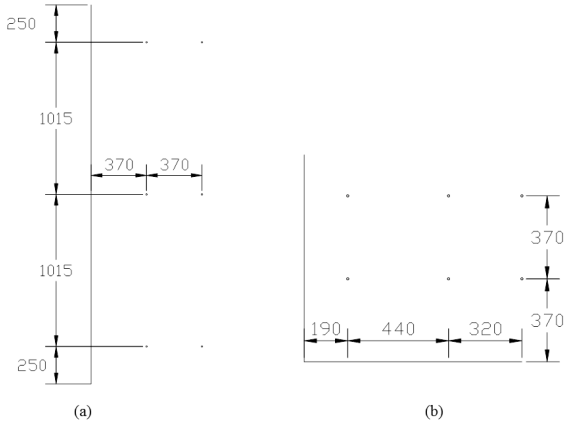

Figure 4. Plan view of measurement locations accessed from (a) the grid bar side of the inlet chute and (b) a side wall of the Plane Creek shredder during the 2017 crushing season. Grid-bar side of the shredder is on the left of the locations in (b).

Figure 5. (a) Side view of the Plane Creek shredder inlet chute after the modifications showing the measurement holes. (b) Plan view of the measurement locations accessed from these measurement holes.

As part of the Plane Creek shredder modifications the casing was replaced, and more insulation was added to the grid bar side of the inlet chute. New holes were drilled in the side walls for the measurements as shown in Figure 5(a) and a plan view of the measurement locations accessed from these holes is shown in Figure 5(b).

Tully

Velocity and static pressure measurements were taken at various locations around the Tully shredder during the 2018 crushing season before and after the installation of the added windage plate. Figure 6 shows a plan view of the velocity measurement locations accessed from the grid bar side wall of the inlet chute.

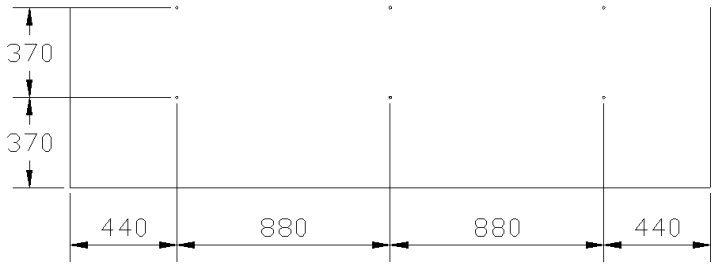

Figure 6. Plan view of the velocity measurement locations accessed from the grid bar side (bottom of figure) of the Tully shredder inlet chute.

Static pressures were measured from the access holes on the grid bar side of the inlet chute. Velocity measurements were also taken at the cane entry of the shredder below the curtain and static pressure measurements were taken from the boot and the side of the prepared-cane elevator.

RESULTS

Plane Creek

Side-elevation views of the predicted air velocity distributions through the Plane Creek shredder before and after the modifications are shown in Figure 7. With the before modifications geometry, a fairly strong recirculation zone was predicted to occur on the grid bar side of the internal baffle. Less intense recirculation was predicted to

occur above and below the kicker. A low velocity recirculation zone was predicted to occur on the cane inlet side of the internal baffle. With the after modifications geometry, the recirculation zones above and below and on the cane inlet side of the kicker were predicted to become more intense. This increase in intensity could be due to the kicker being moved towards the grid bar side of the shredder, leaving more room for the recirculation zones on the cane inlet side of the kicker to develop. Recirculation was still predicted to occur in the inlet chute above the shredder rotor after the modifications, but the recirculation was slightly less intense and occurred over a smaller region.

Close-up side-elevation views of the predicted air velocity distributions through the centreline of the duct work just above the rotor of the Plane Creek shredder are shown in Figure 8. Before the shredder modifications the recirculation on the grid bar side of the internal baffle was anticlockwise and the low velocity recirculation on the cane inlet side of the internal baffle was clockwise. Virtually all the air from the rotating assembly was predicted to enter the recirculation zone on the grid bar side of the internal baffle. With the internal baffle removed and the windage plate installed at the bottom of the inlet chute, less air from around the rotating assembly entered the inlet chute and the air that did enter the inlet chute travelled more towards the grid bar side wall of the inlet chute where it changed direction and then joined the anticlockwise recirculation zone. Note that the plane of view for the plots in Figure 7 and Figure 8 does not pass through the shredder hammer tips, which is why the peak air velocity in all these plots was less than 30 m/s. If the plane of view is adjusted to pass through some of the shredder hammer tips the flow patterns away from the hammer tips are very similar to those in Figures 7-8.

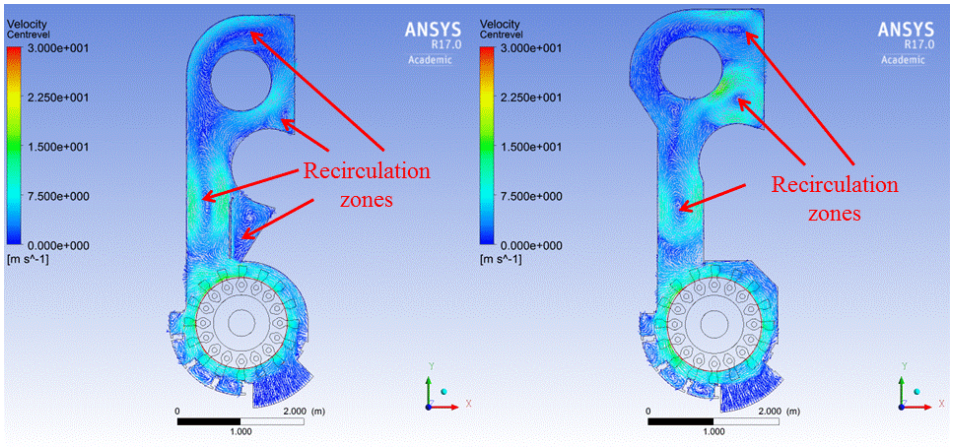

Figure 7. Side-elevation views of the predicted air-velocity distributions through the centreline of the Plane Creek shredder (a) before and (b) after the modifications.

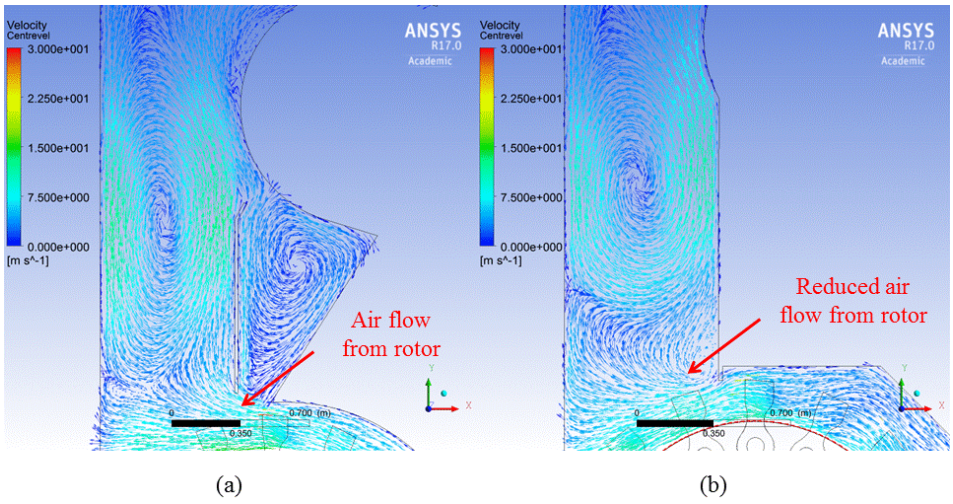

Figure 8. Close-up side-elevation views of the predicted air-velocity distributions through the centreline of the duct work just above the rotor of the Plane Creek shredder (a) before and (b) after the modifications.

The air velocities measured across the width of the Plane Creek shredder inlet chute 370 mm and 740 mm from the grid-bar side wall of the chute during the 2017 crushing season are shown in Table 1. The measurements do not show any consistent velocity distribution across the width of the inlet chute. Closest to the grid-bar side wall the highest velocity was in the centre of the chute but away from the grid-bar side wall and the highest velocity was on one side of the chute. The flows in the inlet chute were quite unsteady. While the velocity magnitudes were measured with a hot-wire anemometer it was difficult to determine the flow direction with this instrument. An L-type pitot was used to determine if the flow was up or down (the flow was up at all points) but the angle of the flow with the vertical could not be determined. Given that the flow domain in the models was only approximately 760 mm wide it was not possible to get meaningful predictions of the velocities across the full width of the inlet chute. The variation in velocities across the inlet chute width seen in Table 1 suggested that the use of symmetry boundary conditions on each side wall of the modelled flow domain was not justified.

Table 1. Measured air velocities (m/s) during the 2017 crushing season at each of the locations accessed from the grid bar side wall of the inlet chute of the Plane Creek shredder (locations shown in Figure 4(a)). Measurements in left column are closest to the grid bar side wall. Positive velocities denote upward flow.

Position	370 mm from grid bar side wall	740 mm from grid bar side wall
2280 mm from side wall	8.2	6.75
1265 mm from side wall	11	4.93
250 mm from side wall	8.1	4.52

Table 2 compares the measured (during the 2017 crushing season) and predicted air velocities from the side wall of the Plane Creek shredder inlet chute. The third and sixth columns of the table correspond to points on the cane-inlet side of the internal baffle. The measurements show upward flow at all locations on the grid-bar side of the internal baffle (first and second columns in the table) and downward flow at all locations on the cane-inlet side of the internal baffle (third column). The predictions show downward flow closest to the wall (column four), upward flow closer to the internal baffle (column five), and small upward flows on the cane inlet side of the internal baffle (column six). The predictions in Table 2 are consistent with the counter rotating recirculation zones seen in Figure 8(a). While the measurements and predictions both have much lower velocities on the cane-inlet side of the internal baffle, the measurements show no indication of the predicted recirculation zone on the grid-bar side of the internal baffle seen in Figure 8(a).

Table 2. Measured air velocities (m/s) during the 2017 crushing season at each of the locations accessed from the side wall of the inlet chute of the Plane Creek shredder compared with predicted velocities (locations shown in Figure 4(b)). Positive velocities denote upward flow.

	Measurements			Predictions		
	190 mm from grid-bar side wall	630 mm from grid-bar side wall	950 mm from grid-bar side wall	190 mm from grid-bar side wall	630 mm from grid-bar side wall	950 mm from grid-bar side wall
740 mm from side wall	14.8	7.5	-0.8	-5.8	5.8	1.3
370 mm from side wall	13.6	10.5	-0.1	-5.8	6.1	0.8

The air-velocity measurements carried out during the 2018 crushing season (after the shredder modifications) through the side-wall access holes are compared with predictions in Table 3. There is reasonably good agreement between the magnitude of the velocity measurements and predictions at the locations closest to the grid-bar side of the inlet chute (columns one and three), but the measured velocities were upward and the predicted velocities were downward. On the cane-inlet side of the inlet chute (columns two and four) the predicted velocities were higher than the measured velocities and both the predicted and measured velocities

were upward. Note that during the 2018 crushing season side-wall measurement locations were approximately 1600 mm higher than the 2017 crushing season side-wall measurement locations (Figure 2). Although it would have been preferable to see downward flows following the modifications, at least the magnitude of the flows was considerably lower.

Table 3. Measured air velocities (m/s) during the 2018 crushing season at each of the locations accessed from the side wall of the inlet chute of the Plane Creek shredder compared with predicted velocities. Positive velocities denote upward flow.

	Measurements		Predictions	
	90 mm from grid-bar side wall	560 mm from grid-bar side wall	90 mm from grid-bar side wall	560 mm from grid-bar side wall
740 mm from side wall	4.2	1.9	-3.8	4.0
370 mm from side wall	3.6	1.8	-3.7	2.9

Tully

Side elevation views of the predicted air velocity distributions through the Tully shredder before and after the installation of the added 180 mm windage plate are shown in Figure 9. In both cases three recirculation zones were predicted in the inlet chute; the largest of these zones was just below the kicker. A large anticlockwise recirculation pattern was predicted to form in the prepared-cane elevator chute for both cases. After the added windage plate was installed the lower two recirculation zones in the inlet chute became slightly less intense but the larger recirculation zone just below the kicker and the recirculation pattern in the cane-elevator chute were unchanged.

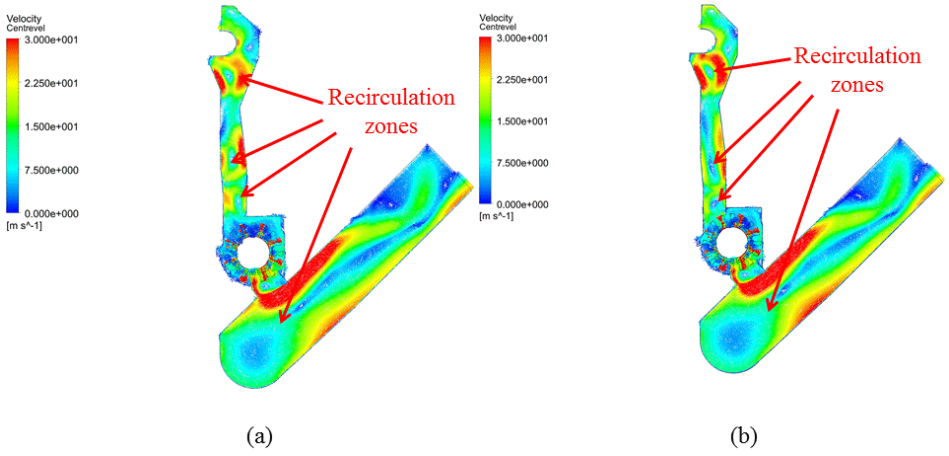

Figure 9. Side-elevation views of the predicted air-velocity distributions through the centreline of the Tully shredder (a) before and (b) after the installation of the windage plate.

Close-up side-elevation views of the predicted air velocity distributions through the centreline of the Tully shredder are shown in Figure 10. For both cases the recirculation in the bottom of the inlet chute was clockwise – opposite to the direction of the recirculation in the Plane Creek shredder-inlet chute. With the added windage plate installed, the intensity of the recirculation in the bottom of the Tully shredder-inlet chute was reduced. Without and with the added windage plate the air entered the shredder from the prepared-cane elevator chute at high velocity (> 30 m/s).

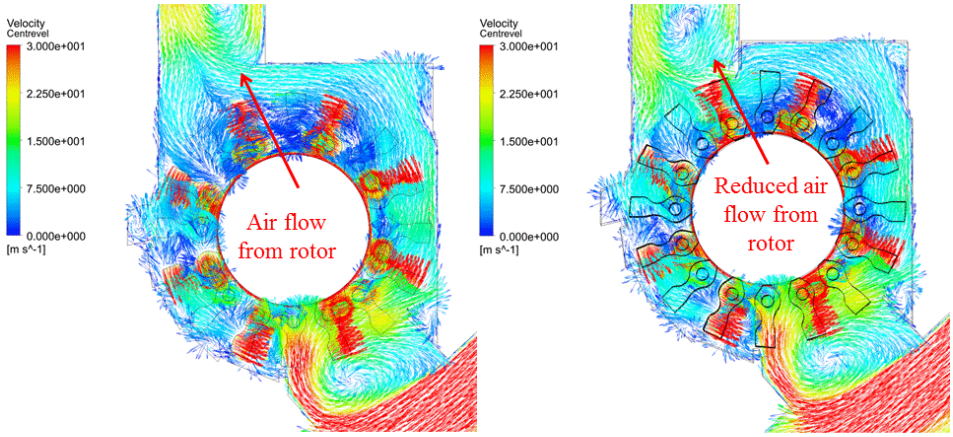

Figure 10. Close-up side-elevation views of the predicted air velocity distributions through the centreline of the Tully shredder (a) before and (b) after the installation of the added windage plate.

Table 4 compares the measured air velocities without and with the added windage plate installed at each of the locations accessed from the grid bar side wall of the Tully shredder-inlet chute. The predictions at the locations on the shredder centreline are also included. The measurements show the added windage plate significantly reduced the air velocities in the inlet chute at all locations. The predicted velocities without the windage plate installed were much higher than the measured velocities. The predicted velocities with the added windage plate installed were also higher than the measured velocities but were much lower than the predicted velocities without the added windage plate installed. Recirculation was predicted without and with the added windage plate installed; downward flow was predicted 370 mm from the grid-bar side wall and upward flow was predicted 740 mm from the grid-bar side wall.

Table 4. Measured air velocities (m/s) during the 2018 crushing season before and after the installation of the added windage plate at each of the locations accessed from the grid bar side wall of the Tully shredder inlet chute (locations shown in Figure 6). Predictions at the locations on the shredder centreline are also included. Measurements in columns one and three and predictions in columns five and seven are closest to the grid-bar side wall. Positive velocities denote upward flow.

	Measurements				Predictions			
	No added plate		With added plate		No added plate		With added plate	
Distance from grid-bar side wall	370	740	370	740	370	740	370	740
2200 mm from side wall	6.5	4.5	-0.8	-2.1				
1320 mm from side wall	6.5	4.5	-1.5	-3.0	-25.0	37.0	-7.4	5.2
440 mm from side wall	6.5	4.5	-2.5	-3.1				

From Table 5 the added windage plate significantly reduced the measured air velocity at the cane inlet from 16.6 m/s outflow to 1.9 m/s inflow. This small air inflow will assist with the flow of billets into the shredder. The predictions show only a small reduction in the air outflow at the cane inlet. The measured pressures in the boot and prepared-cane elevator were small without the windage plate and only increased slightly with the windage plate installed. The predicted static pressures are quite different to the measurements especially for the boot.

Table 5. Measured and predicted air velocities (m/s) and static pressures (Pa) during the 2018 crushing season before and after the installation of the added windage plate at various locations around the shredder.

	Measurements		Predictions	
	No added plate	With added plate	No added plate	With added plate
Air velocity at cane inlet (m/s) - outflow positive	16.6	-1.9	8.0	7.5

Boot static pressure (Pa)	1	30	-475	-585
Prepared cane elevator static pressure (Pa)	1	3	20	65

CONCLUSIONS

The modelling and measurements that we carried out have provided useful information on shredder air-flow patterns. The modelling has been able to predict some of the effects of shredder modifications but underestimated the effect of the windage plate installation on the Tully shredder. The modelling predicted recirculation zones in the inlet chutes of both shredders, but the measurements did not show any clear evidence of recirculation in the inlet chutes. However, it should be noted that it was difficult to measure velocity direction in the inlet chutes and some recirculation may have been occurring.

The internal geometry of a shredder is complex, and it is difficult to evaluate the effectiveness of state-of-the-art CFD modelling techniques without a comprehensive program of air-flow measurements. A comprehensive program of air-flow measurements is difficult to perform in a full-scale shredder without disrupting factory operations because the shredder has to be run with no cane. One possible way forward may be to carry out a program of air flow measurement and CFD modelling on the QUT small-scale shredder.

Although the model predictions gave an improved understanding of the flow patterns that contribute to windage, there are still significant issues with the predictions. The treatment of the air inlet/outlet boundary conditions at the cane inlet needs to be investigated further and some of the modelling approximations may need to be looked at again. Predictions may also be improved with the use of different turbulence models.

ACKNOWLEDGEMENTS

The assistance provided by Simon Levers, Brenton Wood and Elroy Beauzec of Plane Creek Mill and Michael Verri and Paul O'Kane of Tully Mill and the funding support of Sugar Research Australia Limited are gratefully acknowledged.

REFERENCES

Launder B, Spalding D (1972) *Mathematical models of turbulence*. Academic Press, New York.
Mann AP, Plaza F, Bakir CH, Kent GA (2017) Modelling the flows through a shredder. *Proceedings of the Australian Society of Sugar Cane Technologists,* 39, 604–617.